Spectrochimica Acta Part A: Molecular and Biomolecular Spectroscopy 124 (2014) 59–63

Contents lists available at ScienceDirect

Spectrochimica Acta Part A: Molecular and Biomolecular Spectroscopy

journal homepage: www.elsevier.com/locate/saa

A highly selective chemosensor for Al^{3+} based on 2-oxo-quinoline-3-carbaldehyde Schiff-base

Ke Zhang [a], Zheng-yin Yang [a,*], Bao-dui Wang [a,*], Shao-Bo Sun [b], Ying-Dong Li [b], Tian-rong Li [a], Zeng-chen Liu [c], Jun-mei An [a]

[a] College of Chemistry and Chemical Engineering and State Key Laboratory of Applied Organic Chemistry, Lanzhou University, Lanzhou 730000, PR China
[b] Institute of Integrated Traditional and Western Medicine, Gansu University of Traditional Chinese Medicine, Lanzhou 730000, PR China
[c] Department of Chemistry, Zhoukou Normal University, Zhoukou 466001, PR China

HIGHLIGHTS

- The new Schiff-base ligand (**1**) was easily synthesized and widely available.
- The compound **1** exhibited a high selectivity and sensitivity toward Al^{3+} in ethanol.
- The detection limit of **1** to Al^{3+} was up to 0.67 ppb.
- Potential utilization of **1** as intracellular sensors of Al^{3+} ions was also examined.

GRAPHICAL ABSTRACT

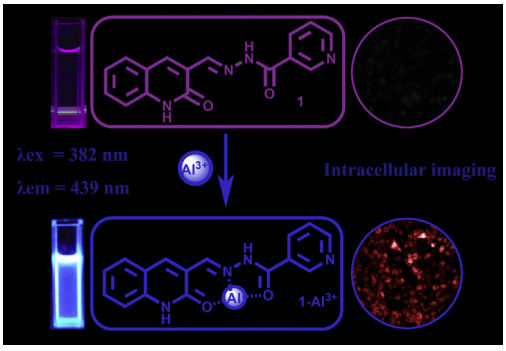

ARTICLE INFO

Article history:
Received 30 August 2013
Received in revised form 6 December 2013
Accepted 11 December 2013
Available online 4 January 2014

Keywords:
Fluorescence chemosensors
Sensitivity and selectivity
Quinoline derivatives
Detection limit
Bioactivity of Al^{3+} in living cells

ABSTRACT

A new Schiff-base ligand (**1**) with good fluorescence response to Al^{3+}, derived from 2-oxo-quinoline-3-carbaldehyde and nicotinic hydrazide, had been synthesized and investigated in this paper. Spectroscopic investigation revealed that the compound **1** exhibited a high selectivity and sensitivity toward Al(III) ions over other commonly coexisting metal ions in ethanol, and the detection limit of Al^{3+} ions is at the parts per billion level. The mass spectra and Job's plot confirmed the 1:1 stoichiometry between **1** and Al^{3+}. Potential utilization of **1** as intracellular sensors of Al^{3+} ions in human cancer (HeLa) cells was also examined by confocal fluorescence microscopy.

Introduction

Fluorescence probes, especially quinoline-based structures, play a crucial role in bioimaging studies [1,2]. Recently, many studies used quinoline scaffolds as central caged or fluorescence chemical cores to investigate small endogenous molecule functions [3–6]. To be efficient, these fluorescent probes should be biocompatible and have optimal fluorescent properties. In this context, quinolines appear quite attractive due to their relative synthetic versatility. The facile introduction of substituents to quinoline heterocyclic scaffold allows subsequent tuning of physicochemical properties of molecules (fluorescence, solubility, etc.) [7]. Syntheses of substituted quinolines have been reported using various mechanisms and strategies: Conrad–Limpach–Knorr [8], Skraub–Doebner–Von Miller [9–11], Frielaender [12,13], halogen mediated [14], copper catalyzed [15] or miscellaneous [10,16].

* Corresponding authors. Tel.: +86 9318913515; fax: +86 9318912582.
E-mail addresses: yangzy@lzu.edu.cn (Z.-y. Yang), wangbd@lzu.edu.cn (B.-d. Wang).

1386-1425/$ - see front matter © 2013 Elsevier B.V. All rights reserved.
http://dx.doi.org/10.1016/j.saa.2013.12.076

Up to now, many fluorescent chemosensors based quinoline derivatives have been reported [17]. However, only a few chemosensors can distinguish Al^{3+} in the biotic environment. Meanwhile, many fluorescent chemosensors based on Schiff-base have been designed and investigated owing to the simplicity and sensitivity of Schiff-base type fluorescence sensors [18]. Due to the low density and the passivate phenomenon of aluminum, it has been widely used in many fields, such as aerospace industry, automobile manufacturing, computers, food additions, aluminum-based pharmaceuticals and storage/cooking utensils [19–23]. The moderate increasing of concentration of Al^{3+} in organicnism, which may lead to various physiological diseases, such as Alzheimer's disease and osteoporosis [24–27]. However, the heightened concern for environmentally and biologically relevant species of Al^{3+} has stimulated active research on the potential impact of its toxic effects [28]. According to a WTO report, the average daily human intake of aluminum is approximately 3–10 mg per day [29]. Simultaneously, the aluminum toxicity also renders almost 40% of the acidic soils in the world [30–32]. In consideration of the potential impact of Al^{3+} in human health and the environment, highly selective and sensitive chemosensors of Al^{3+} are widely needed.

Hence, we report a novel bis Schiff-base fluorescent sensor (**1**) derived from 2-oxo-quinoline-3-carbaldehyde and nicotinic hydrazide. As a new fluorescent sensor for Al^{3+}, the complex exhibits a high sensitivity and selectivity. At the same time, sensitive bioimaging of Al^{3+} in the cell is a prerequisite for understanding the underlying mechanism about how aluminum ions function during aluminum-induced human diseases. Herein, in order to detect the application of the complex in the biotic environment, we design a Schiff base (**1**) probe named **2-oxo-quinoline-3-carbaldehyde** (**nicotinoyl**) **hydrazone** which enhances fluorescence upon binding to Al^{3+} with high selectivity. The detection limit of Al^{3+} ions is at the parts per billion level in EtOH solution. Potential utilization of **1** as intracellular sensors of Al^{3+} in human cancer (HeLa) cells was also examined by confocal fluorescence microscopy.

Experimental section

Materials and instrumentation

The chemicals for synthesis were purchased from Aladdin-reagent (China). 2-oxo-quinoline-3-carbaldehyde was prepared according to the literature [33,34]. All the used metal ions were prepared with nitrate salts. All the materials and solvents were of analytical reagent grade quality and used without further purification.

^{1}H NMR spectra were recorded on a Varian 400-MHz instrument with DMSO-d_6 as solvent. ESI-MS spectra were determined with a Bruker Esquire 6000 spectrometer. UV–vis absorption spectra were obtained with a Perkin Elmer Lambda 35 UV–vis spectrophotometer and recorded in quartz cells with 1 cm optical path length. Fluorescence spectra were acquired on a Hitachi RF-4500 fluorescence spectrophotometer and equipped with quartz cuvettes of 1 cm path length. Infrared spectra were measured with KBr disks on a Therrno Mattson FTIR spectrometer in the 4000–400 cm^{-1}. The melting points of the compounds were determined on a Beijing XT4-100x microscopic melting point apparatus. The Cytotoxicity Assay was detected by a microplate reader (Nanjing Huadong Electronics Group Co., Ltd. DG5033A – microplate reader). The Intracellular imaging were illuminated under a Zeiss Leica inverted epifluorescence/reflectance laser scanning confocal microscope.

Synthesis of 2-oxo-quinoline-3-carbaldehyde (nicotinoyl) hydrazone (1)

As shown in Scheme S1, 2-oxo-quinoline-3-carbaldehyde was prepared according to the literature [33,34]. An ethanol solution containing Nicotinic hydrzide (0.274 g, 2 mmol) was added to another ethanol solution containing 2-oxo-quinoline-3-carbaldehyde (0.344 g, 2 mmol). The mixture was magnetically stirred and refluxed for 5 h and then cooled to room temperature by removing the heat source. A yellow material was precipitated

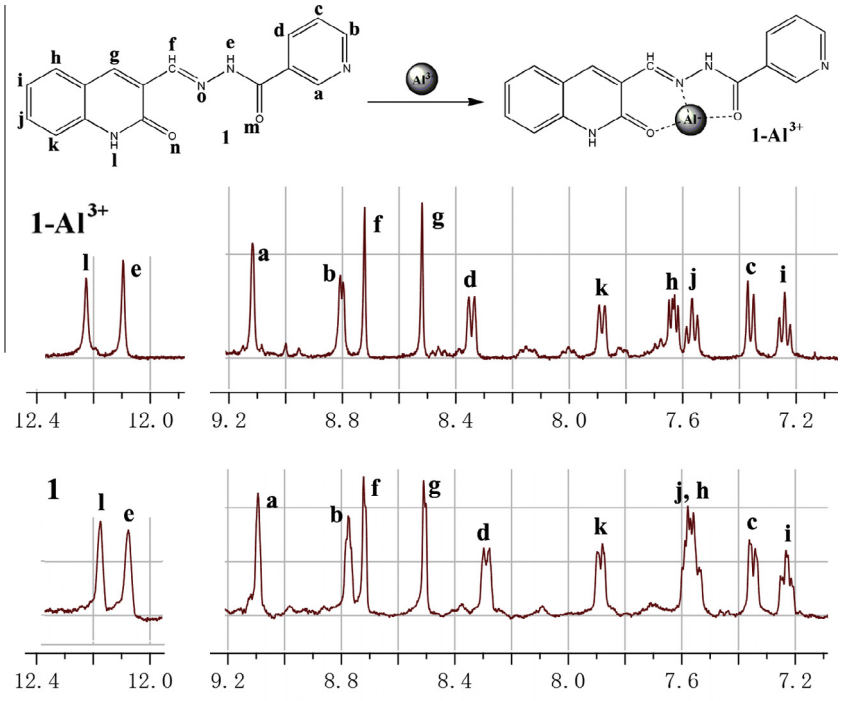

Fig. 1. The ^{1}H NMR titration of **1** and **1** – Al^{3+} in DMSO-d_6 at room temperature.

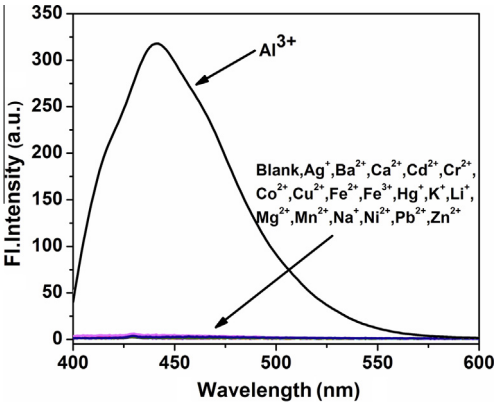

Fig. 2. Fluorescence spectra (excitation at 382 nm) of 1 (10 μM) at 25 °C in EtOH in the presence of 2 equivalent of Al^{3+}, Li^{+}, Na^{+}, K^{+}, Mg^{2+}, Ca^{2+}, Ba^{2+}, Pb^{2+}, Cr^{3+}, Mn^{2+}, Fe^{2+}, Fe^{3+}, Co^{2+}, Ni^{2+}, Cu^{2+}, Ag^{+}, Zn^{2+}, Cd^{2+} and Hg^{2+}. Slit: excitation/emission = 3.0:3.0.

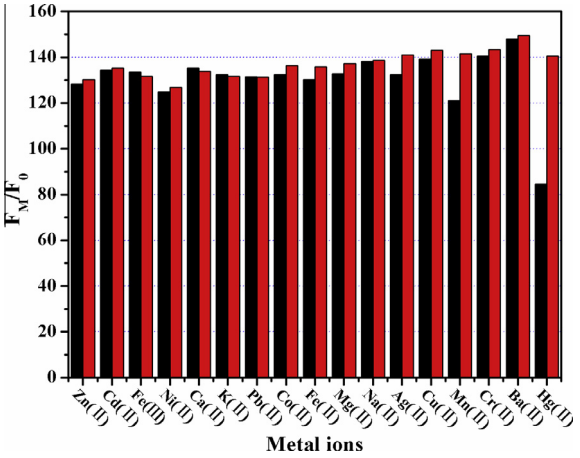

Fig. 3. Competitive binding experiments of **1** in which the Al^{3+} (20.0 μM) (red bars) were added to the solution of **1** (10.0 μM) followed by competing metal ions (20.0 μM) (black bars) in **EtOH**. (For interpretation of the references to colour in this figure legend, the reader is referred to the web version of this article.)

and separated via vacuum filtration, washed three times with hot ethanol, and recrystallized from ethanol. A yield of 65% was obtained. Mp > 300 °C. ^{1}H NMR (400 MHz, DMSO-d_6): δ (ppm) 12.161(s, 1H); 12.059(s, 1H); 9.091(s, 1H); 8.769–8.778(d, J = 3.6 Hz, 1H); 8.719(s, 1H); 8.504(s, 1H); 8.277–8.297(d, J = 8.0 Hz, 1H); 7.874–7.894(d, J = 8.0 Hz, 1H); 7.537–7.593(m, J = 22.4 Hz, 2H); 7.339–7.360(d, J = 8.4 Hz, 1H); 7.211–7.248(t, J = 4.8 Hz, 1H); IR: 3857, 3744, 3202–2885, 1655, 1556, 1425, 1274, 1142, 957, 858, 754, 704, 459; ESI-MS m/z: 293.2 ($[M + H]^+$).

Optical detection of metal ions with 1

The sensor **1** (10.0 μM) was mixed with different concentrations of metal ions in EtOH in a 1 cm cell. Solutions of metal ions were prepared by using nitrate salts. After equilibrium at ambient temperature for 3 min, fluorescence spectra of the mixtures were measured. The excitation wavelength was at 382 nm.

Cytotoxicity assay and Intracellular imaging

In vitro cytotoxicity of the **1** was evaluated by performing methyl thiazolyl tetrazolium (MTT) assay of the HeLa cells incubated with the probe. Cells were seeded into a 96-well cell culture plate with a density of 5×10^4 cells/well in DMEM with 10% FBS at 37 °C under 5% CO_2 for 24 h. Then, the cells were incubated with **1** and Al^{3+} with different concentrations (0, 5, 10, 20, 40, 80 and 100 mmol/mL in DMEM) for 24 h, respectively at 37 °C under 5% CO_2. Thereafter, in the addition of MTT (20 mL, 5 mg/mL) to each well, the plate was incubated for 4 h at 37 °C. After the addition of dimethyl sulfoxide(DMSO, 100 μL/well), the cell plate was allowed to stand at 37 °C for 10 min. The optical density was measured at 490 nm using a microplate reader (Nanjing Huadong Electronics Group Co., Ltd. DG5033A – microplate reader). To detect if sensor **1** can be used to fluorescently visualize intracellular Al^{3+}, the HeLa cell was cultured in Dulbecco's Modified Eagle's medium (DMEM) supplemented with 20 μM **1** and 10% fetal bovine serum at 37 °C for 5 h, then the cells were washed twice with PBS (1 mL) and illuminated under a Zeiss Leica inverted epifluorescence/reflectance laser scanning confocal microscope.

Result and discussion

NMR titration

NMR spectroscopy was used to elucidate the structure of **1** and the binding mode of **1** and Al^{3+}. As shown in Fig. 1, the ^{1}H NMR spectra of **1** and 1 – Al^{3+} complexes provided obvious changes of chemical shifts. After the addition of Al^{3+}, O_m, O_n and N_o participated in the coordination. On account of the conjugated structure, the H_a, H_b and H_d shifted to a higher field about 0.03 ppm, 0.06 ppm and 0.05 ppm, respectively, and the shift of H_c was weak since the meta-position. This proved that the O_m atom have taken part in coordination to Al^{3+} ion. Meanwhile, H_f and H_g shifted to a higher field, H_h become separated to H_j compared with the ^{1}H NMR spectra of **1**, and H_i, H_j and H_k had little shift, which means O_n and N_o provided their lone pair electrons to coordinated with Al^{3+}. The active hydrogens H_e and H_l also shifted to a higher field about 0.05 ppm. Those dramatic changes in the ^{1}H NMR titration fully proved the binding mode of **1** and Al^{3+}.

Fluorescence spectra

The optical properties of **1** and its coordination compound were mainly investigated by fluorescence emission spectra in EtOH. As shown in Fig. 2, the fluorescence spectra (λ_{ex} = 382 nm) of 1 (10 μM) measured in EtOH solution in the presence of different metal ions (2 equiv). The related alkali, alkaline earth and other

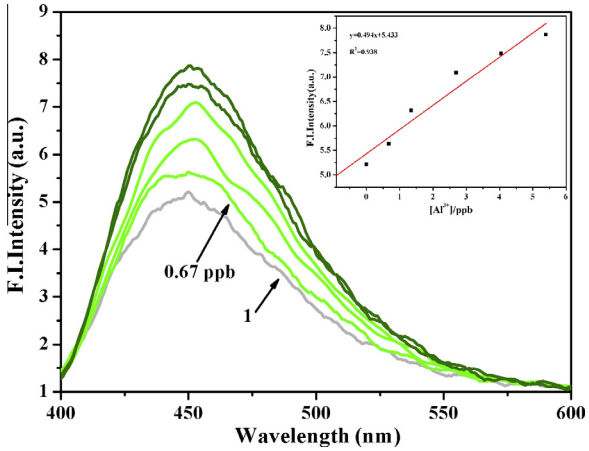

Fig. 4. The determination limit of **1** for Al^{3+} was obtained by fluorescence spectra (excitation at 382 nm). Inset: Al^{3+} concentration (at the parts per billion level) dependent fluorescence intensity change.

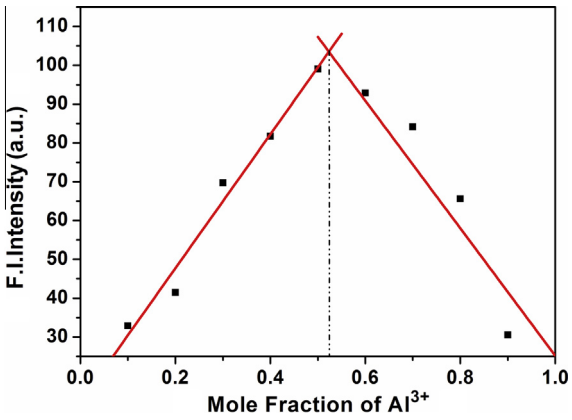

Fig. 5. Job's plot for the complexation of **1** with Al^{3+} in EtOH solution. $[1] + [Al^{3+}] = 2 \times 10^{-5}$ M.

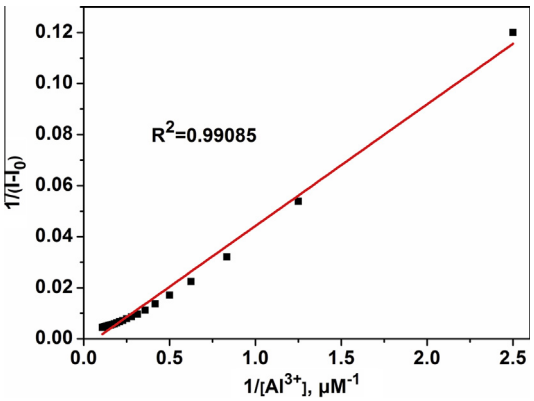

Fig. 6. Benesi–Hildebrand analysis of the emission changes for the complexation between **1** and Al^{3+}.

traditional metal ions such as Li^+, Na^+, K^+, Mg^{2+}, Ca^{2+}, Ba^{2+}, Pb^{2+}, Cr^{3+}, Mn^{2+}, Fe^{2+}, Fe^{3+}, Co^{2+}, Ni^{2+}, Cu^{2+}, Ag^+, Zn^{2+}, Cd^{2+} and Hg^{2+} were taken into consideration. After the addition of Al^{3+}, sensor **1** showed a sharp fluorescence emission at around 439 nm, and the fluorescence intensity was significantly enhanced by approximately 150-fold. On the contrary, sensor **1** showed very weak fluorescence in the presence of the respective ions beside Al^{3+}.

Furthermore, the competition experiments have been performed. **1** was mixed with 2 equiv of Al^{3+} in the presence of the same amount of the above-mentioned metal ions.

Fig. 3 shows the fluorescence changes of **1** after the addition of the other ions. Apparently, most of the examined metal ions caused negligible changes in the fluorescence emission spectra except for Hg^{2+} and Mn^{2+}. The Hg^{2+} and Mn^{2+} quenches the fluorescence of chemsensor **1** because of the stronger binding abilities than Al^{3+}. While in the presence of those competing ions, the Al^{3+} nonetheless led to a prominent fluorescence enhancement. Thus, **1** can be used as an Al^{3+} selective fluorescence sensor in the presence of most common metal ions.

Moreover, the detection limit of sensor **1** was likewise examined. Separate volumes of Al^{3+} (10^{-7} M) between 0 and 40 μL were added to the sensor **1** solution, respectively. We observed that the fluorescence emission of **1** could be unambiguously distinguished from the mixed solution by the added Al^{3+} (5 μL). The detection limit of Al^{3+} ions was up to 0.67 ppb, which was inferior to the limit of Al^{3+} in drinking water (0.05–0.2 mg/L) set by the US Environment Protection Agency (EPA). It is indicated that compound **1** had highly sensitive toward Al^{3+} (see Fig. 4).

The structure between sensor **1** and Al^{3+} was discussed through fluorescence titration, Job's plot and Mass spectra. As depicted in the Job's plot (Fig. 5), the fluorescence intensity reached the maximum value when the mole fraction of Al^{3+} reached 0.5, the linear relation probed that Al^{3+} and **1** form the **1**-Al^{3+} complex with the binding mode of 1:1. The mass spectra of the **1**-Al^{3+} coordination compound further confirmed the 1:1 stoichiometry of **1**-Al^{3+}. According to the binding isotherm of the fluorescence titration (Fig. S1), the fluorescence intensity was increased steadily along with the addition of Al^{3+}. However, we did not acquired the saturation of Al^{3+} due to the slowly rate of the reaction between Al^{3+} and **1**.

In addition, the Benesi–Hildebrand method was used to demonstrate the structure between **1** and Al^{3+}. Fig. 6 shows the B-H plot of **1**-Al^{3+}, the linear relation also probed that Al^{3+} and **1** showed a 1:1 stoichiometry. At the same time, we could estimate the binding constant of **1**-Al^{3+} complex.

Where I_0 is the integrated fluorescence intensity of a free sensor, I is the observed integrated fluorescence intensity, and [M] is the metal ion concentration. When $1/(I - I_0)$ is plotted against 1/[M], the binding constant is given by the intercept/slope ratio. From curve fitting of sensor **1** fluorescence intensity against the reciprocal of the Al^{3+} concentration ($1/[Al^{3+}]$), this Benesi–Hildebrand

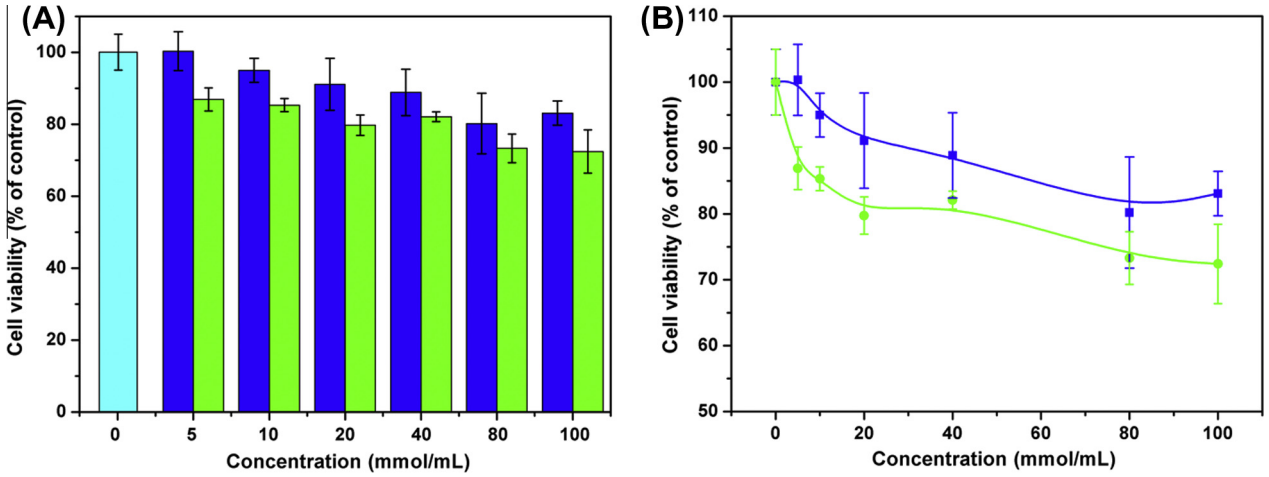

Fig. 7. In vitro cell viability of Hela cells incubated with **1** (blue bars) and Al^{3+} (green bars) with different concentrations (0, 5, 10, 20, 40, 80 and 100 mmol/mL) incubated for 24 h at 37 °C. (For interpretation of the references to colour in this figure legend, the reader is referred to the web version of this article.)

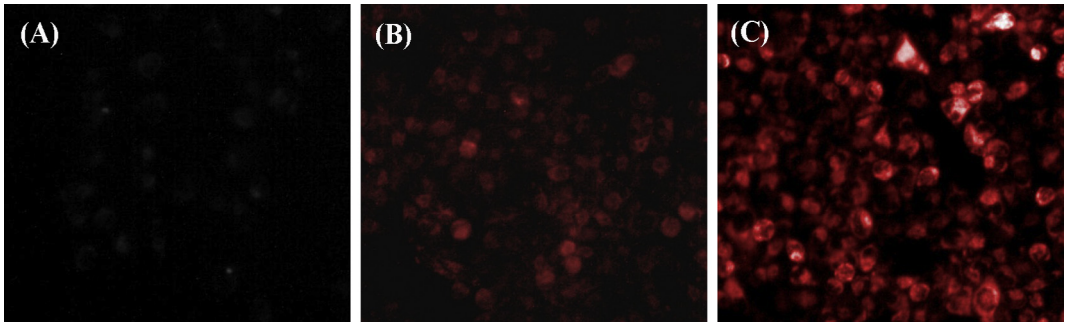

Fig. 8. Fluorescent images of **1** in the addition of Al^{3+} in HeLa cells. (A) Fluorescence image of HeLa cells incubated with **1** (20 μM). (B) Fluorescence image of HeLa cells incubated with 5 μM $Al(NO_3)_3$ for 5 h and exposed with **1** (20 μM). (C) 20 μM $Al(NO_3)_3$ for 5 h and exposed with **1** (20 μM).

plot yielded a linear fit (Fig. 6), from which the K_d value was estimated to be 69.99 mM. The linear fit also evidenced the 1:1 complexation behavior.

Cytotoxicity assay

To detected the application of sensor **1**, the cytotoxicity of the particles was evaluated via an MTT [3-(4, 5-dimethylthiazol-2-yl)-2, 5-diphenyltetrazolium bromide] assay of the viability of the HeLa cell line. As shown in Fig. 7, no obvious decrease in cell viability was observed after the cells were incubated with **1** and Al^{3+} with various concentrations of **1** for 24 h, which is essential for further biological applications.

Intracellular imaging

Subsequent experiment was conducted to detect if sensor **1** can be used to fluorescently visualize intracellular Al^{3+}. The intracellular imaging reveals no fluorescence as determined by laser scanning confocal microscopy (Fig. 8A). Cells were subsequently incubated with 5 μM Al^{3+} at 37 °C for 5 h under the same conditions, whereupon a significant increase in the fluorescence was observed (Fig. 8B). The fluorescence image grew brighter as the concentration of Al^{3+} increased (Fig. 8C). These results demonstrate that sensor **1** is permeable to cells, binds to intracellular Al^{3+}, and emits fluorescent light upon binding to the metal ion. It should therefore be potentially useful for the study of the toxicity or bioactivity of Al^{3+} in living cells.

Conclusion

In summary, we describe the syntheses, properties, and application in Intracellular imaging of a novel fluorescent chemosensor (**1**) based on a bis Schiff-base ligand, derived from 2-oxo-quinoline-3-carbaldehyde and Nicotinic hydrazide. Spectroscopic investigation revealed that the compound exhibited a high selectivity and sensitivity toward Al(III) ions over other commonly coexisting metal ions in EtOH solution. After the addition of Al^{3+} into the solution of sensor **1**, the fluorescence was markedly enhanced by approximately 150-fold at around 439 nm. The detection limit of Al^{3+} ions was up to 0.67 ppb. Moreover, confocal microscopy experiments established that sensor **1** can be used for detecting Al^{3+} in living cells, which indicated its potential applications for biological toxicities.

Acknowledgements

The work was supported by the National Natural Science Foundation of China (81171337), the NCET (13-0262) and the Fundamental Research Funds for the Central Universities (lzujbky-2013-56).

Appendix A. Supplementary material

Supplementary data associated with this article can be found, in the online version, at http://dx.doi.org/10.1016/j.saa.2013.12.076.

References

[1] R.L. Sheng, P.F. Wang, Y.H. Gao, Y. Wu, W.M. Liu, J.J. Ma, H.P. Li, S.K. Wu, Org. Lett. 10 (2008) 5015–5018.
[2] H.S. Jung, P.S. Kwon, J.W. Lee, J.I. Kim, C.S. Hong, J.W. Kim, S.H. Yan, J.Y. Lee, J.H. Lee, T. Joo, J.S. Kim, J. Am. Chem. Soc. 131 (2009) 2008–2012.
[3] S. Kantevari, M. Matsuzaki, Y. Kanemoto, H. Kasai, G.C.R. Ellis Davies, Nat. Methods 7 (2009) 123–125.
[4] J. Gordo, J. Avo, A.J. Parola, J.C. Lima, A. Pereora, P.S. Brance, Org. Lett. 13 (2011) 5112–5115.
[5] G. Jones, W.R. Jackson, C.Y. Choi, W.R. Bergmark, J. Phys. Chem. 89 (1985) 294–300.
[6] R.S. Koefod, K.R. Mann, Inorg. Chem. 28 (1989) 2285–2290.
[7] Y. Laras, V. Hugues, Y. Chandrasekaran, M. Blanchard-Descs, F.C. Acher, N. Pietrancosta, J. Org. Chem. 77 (2012) 8294–8302.
[8] F. Misani, M.T. Bogert, J. Org. Chem. 10 (1945) 347–365.
[9] N. Sakai, D. Aoki, T. Hamajima, T. Konakahara, Tetrahedron Lett. 47 (2006) 1261–1265.
[10] Y.C. Wu, L. Liu, H.J. Li, D. Wang, Y.J. Chen, J. Org. Chem. 71 (2006) 6592–6595.
[11] J.J. Eisch, T. Dluzniewski, J. Org. Chem. 54 (1989) 1269–1274.
[12] S.V. Ryabukhin, V.S. Naumchik, A.S. Plaskom, O.O. Grygorenko, A.A. Tomachev, J. Org. Chem. 76 (2011) 5774–5781.
[13] S. Gladiali, G. Chelucci, M.S. Mudadu, M.A. Gastaut, R.P. Thummel, J. Org. Chem. 66 (2001) 400–405.
[14] X.X. Zhang, T.L. Yao, M.A. Campo, R.C. Larock, Tetrahedron 66 (2010) 1177–1187.
[15] X.J. Li, Z.J. Mao, Y.G. Wang, W.X. Chen, X.F. Lin, Tetrahedron 67 (2011) 3858–3862.
[16] A. Chaskar, V. Padalkar, K. Phatangare, B. Langi, C. Shah, Taylor & Francis 40 (2010) 2336–2340.
[17] H.Y. Li, S. Gao, Z. Xi, Inorg. Chem. Commun. 12 (2009) 300–303.
[18] P. Roy, K. Dhara, M. Manassero, P. Banerjee, Inorg. Chem. Acta 362 (2009) 2927–2932.
[19] J. Barcelo, C. Poschenrieder, Exp. Bot. 48 (2002) 75–92.
[20] J.R. LakoWicz, Kluwer Academic Publishers, New York, Topics in fluorescence spectroscopy. 4 (2002).
[21] A.P. de Silva, H.Q. Gunaratne, T Gunnlauqsson, A.J. Huxley, C.P. McCoy, J.T. Rademacher, T.E. Rice, Chem. Rev. 97 (1997) 1515–1566.
[22] B. Valeur, I. Leray, Coord. Chem. Rev. 205 (2000) 3–40.
[23] S. Kim, J.Y. Noh, K.Y. Kim, J.H. Kim, H.K. Kang, S.W. Nam, S.H. Kim, S. Park, C. Kim, J. Kim, Inorg. Chem. 51 (2012) 3597–3602.
[24] P. Nayak, Environ. Res. 89 (2002) 101–115.
[25] C.S. Cronan, W.J. Walker, P.R. Bloom, Nature 324 (1986) 140–143.
[26] G. Berthon, Coord. Chem. Rev. 228 (2002) 319–341.
[27] A.M. Pierides, W.G. EdWards Jr., U.X. Cullum Jr., J.T. McCall, H.A. Ellis, Kidney Int. 18 (1980) 115–124.
[28] Y. Lu, S.S. Huang, Y.Y. Liu, S. He, L.C. Zhao, X.S. Zeng, Org. Lett. 13 (2011) 5274–5277.
[29] Z. Krejpcio, R.W. Wójciak, Pol. J. Environ. Stud. 11 (2002) 251–254.
[30] T.P. Flaten, M. Ødegärd, Food Chem. Toxical. 26 (1988) 959–960.
[31] J. Ren, H. Tian, Sensors. 7 (2007) 3166–3178.
[32] R.A. Yokel, Neurotoxicology 21 (2000) 813–828.
[33] M.K. Singh, A. Chandra, B. Singh, R.M. Singh, Tetrahedron Lett. 48 (2007) 5987–5990.
[34] P.K. Kalita, B. Baruah, P.J. Bhuyan, Tetrahedron Lett. 47 (2006) 7779–7782.